

Isochoric Heating of Solid-Density Matter with an Ultrafast Proton Beam

P. K. Patel,¹ A. J. Mackinnon,¹ M. H. Key,¹ T. E. Cowan,² M. E. Foord,¹ M. Allen,¹ D. F. Price,¹ H. Ruhl,²
P. T. Springer,¹ and R. Stephens³

¹Lawrence Livermore National Laboratory, Livermore, California 94550, USA

²Department of Physics/220, University of Nevada-Reno, Reno, Nevada 89507, USA

³General Atomics, P.O. Box 85608, San Diego, California 92186, USA

(Received 14 May 2003; published 19 September 2003)

A new technique is described for the isochoric heating (i.e., heating at constant volume) of matter to high energy-density plasma states ($>10^5$ J/g) on a picosecond time scale (10^{-12} sec). An intense, collimated, ultrashort-pulse beam of protons—generated by a high-intensity laser pulse—is used to isochorically heat a solid density material to a temperature of several eV. The duration of heating is shorter than the time scale for significant hydrodynamic expansion to occur; hence the material is heated to a solid density warm dense plasma state. Using spherically shaped laser targets, a focused proton beam is produced and used to heat a smaller volume to over 20 eV. The technique described of ultrafast proton heating provides a unique method for creating isochorically heated high-energy density plasma states.

DOI: 10.1103/PhysRevLett.91.125004

PACS numbers: 52.50.Gj, 52.27.Gr, 52.38.Ph, 52.57.Kk

Today's generation of ultrahigh-power lasers have the ability to compress and heat matter to energy densities similar to those at the centers of stars, giving them a leading role in the laboratory investigation of extreme states of matter, with major applications in planetary and stellar astrophysics [1] and fusion energy research [2]. Laboratory studies of plasmas enable measurements of fundamental material properties—such as the equation of state and opacity—needed to formulate and benchmark theoretical plasma models [3–6]. Ideally such measurements would be made on uniformly heated plasmas in a single-density and single-temperature state. However, the production of plasmas in such idealized states is rather problematic because the heating or energy deposition is required to be both extremely rapid and uniform throughout the material—that is, isochoric heating, or heating at constant volume, is required. Established methods for volumetric heating such as laser-driven shock heating [7], x-ray heating [8,9], and ion heating [10] while relatively fast (10^{-9} – 10^{-6} sec) are still longer than the typical time scales over which significant hydrodynamic expansion can occur (10^{-12} – 10^{-11} sec). Direct heating with intense subpicosecond laser pulses (10^{-12} sec) is possible but results in highly nonuniform heating due to the laser absorption being localized within a skin depth (<100 nm) of material [11]. In this Letter we present a new approach to the heating of dense plasma states which overcomes both of these problems. This method uses an intense, collimated, laser-generated proton beam to volumetrically heat solid density material to warm dense states on a picosecond time scale.

The discovery that intense, highly directional proton beams could be generated during the interaction of an ultraintense laser pulse with a solid target was made relatively recently [12,13]. These and subsequent experi-

ments characterizing the proton beams have revealed a unique combination of properties including peak proton energies of 55 MeV, conversion efficiencies ranging between 2% and 7%, a temporal duration of <5 ps, and a narrow half-cone angle of emission of 15° – 20° [13–15]. A high-intensity subpicosecond laser pulse incident on a thin Al foil ponderomotively accelerates electrons from the interaction region into the target with relativistic energies. The electrons emerging at the rear surface induce a large electrostatic charge separation field, which in turn accelerates positive ions—mostly protons from a hydrocarbon contaminant layer—from the rear surface to multi-MeV energies, over a distance of a few microns. The protons are accelerated from the rear surface in a well-defined, highly directional beam normal to the target [16,17]. Simulations have shown that by curving the target rear surface the proton beam could potentially be focused to a far higher energy density [17]. This Letter describes the application of an ultrashort-pulse proton beam to volumetrically heat a solid density material to a 4 eV plasma state. The material, a $10\ \mu\text{m}$ thick Al foil, is isochorically heated by the protons at solid density on a few picoseconds time scale—a time over which negligible hydrodynamic expansion of the plasma occurs. In addition, a technique is demonstrated for focusing the proton beam to even higher flux densities. This technique leads to the heating of a smaller volume of solid material to over 20 eV in temperature.

The experiments were performed on the 100 TW JanUSP laser at Lawrence Livermore National Laboratory. JanUSP is a titanium sapphire (Ti:S) laser operating at a wavelength of 800 nm and delivering 10 J of energy in a 100 fs duration pulse [18]. The laser is focused by an $f/2$ off-axis parabola to a $5\ \mu\text{m}$ FWHM (full width at half maximum) spot. For these experiments the laser spot was defocused at the target plane

to a $50\ \mu\text{m}$ diameter with an average intensity of $5 \times 10^{18}\ \text{W cm}^{-2}$ in order to optimize the proton beam for this application. The proton beam was characterized using a stack of 20 sheets of radiochromic film (RCF) placed 25 mm behind a $20\ \mu\text{m}$ thick Al foil target. RCF is an absolutely calibrated dosimetry film measuring total radiation dose or deposited energy. The recorded images show the angular pattern of the beam in the narrow proton energy band depositing energy in each sheet of film. By structuring the rear surface of the Al foil an intensity variation was imprinted on the proton beam [19] which provided a measurement of the size of the emitting region on the foil. The source diameter ranged from 250 to $80\ \mu\text{m}$ for the recorded range of proton energies from 4 to 12 MeV, and was much larger than the laser focal spot. This appears consistent with reflux spreading of the electrons within the target [15]. For the subsequent heating and focusing parts of the experiment a $10\ \mu\text{m}$ thick Al foil with a smooth rear surface was used to generate the proton beam. The energy spectrum of the protons, measured with RCF, was close to an exponential with a temperature of $1.5 \pm 0.2\ \text{MeV}$ and a total energy of 0.1–0.2 J, or 1%–2% of the incident laser energy.

Figure 1(a) shows the experimental setup and target geometries. A planar case was studied first in which the proton beam is produced from a $10\ \mu\text{m}$ planar Al foil, and a second $10\ \mu\text{m}$ Al foil is placed behind the first at a distance of $250\ \mu\text{m}$. In the focusing case the proton beam is produced from a $10\ \mu\text{m}$ thick, $320\ \mu\text{m}$ diameter hemispherical Al shell, and a second $10\ \mu\text{m}$ Al foil is placed in a plane coinciding with the geometric center of the shell. The temperature of the proton heated foil was determined with a fast optical streak camera recording

Planckian thermal emission from the hot rear surface. An absolute single wavelength measurement was made using a $570\ \text{nm}$ interference filter. The overall temporal and spatial resolution was 70 ps and $5\ \mu\text{m}$, respectively. The $10\ \mu\text{m}$ thick proton heated foil blocked any direct light from the primary laser-irradiated target.

The streak camera data obtained for the two target geometries, each with 10 J of laser energy incident on target, are shown in Fig. 1(b). For the planar foil case (left image) we observe quite uniform emission from a large area of the secondary foil ($186\ \mu\text{m}$ FWHM). The onset of the emission is rapid — shorter than the time resolution of the streak camera — and decreases slowly over the following 800 ps. This temporal behavior (a rapid rise with a slow falloff) is consistent with that from a body which is heated isochorically to some temperature and which then under its own pressure expands and cools. The spatial extent of $186\ \mu\text{m}$ is in good agreement with our measurement of the maximum proton source size of approximately $250\ \mu\text{m}$ at the lowest recorded proton energy (N.B. the protons primarily responsible for the heating at a depth of $10\ \mu\text{m}$ have energies in a band around 0.9 MeV). With the hemispherical foil (right image) we observe a dramatic reduction in the size of the heated region ($46\ \mu\text{m}$ FWHM) coupled with a marked increase in the emission intensity (approximately a factor of 8). The factor of 4 reduction in the spatial extent in one dimension corresponds to a 16 times smaller heated area.

An interferometer was used to simultaneously monitor the foils for signs of plasma formation. The interferometry beam was a frequency-doubled 100 fs pulse directed along the target surface and timed to arrive 180 ps after the main pulse. Figure 2 shows the

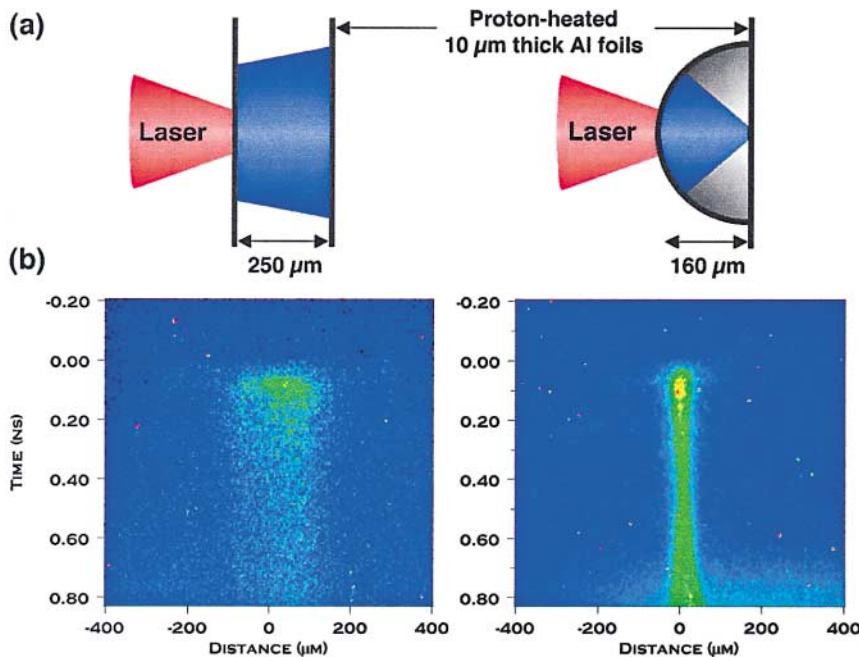


FIG. 1 (color). (a) Experimental setup for flat and focusing target geometries. Each target consists of a flat or hemispherical $10\ \mu\text{m}$ thick Al target irradiated by the laser, and a flat $10\ \mu\text{m}$ thick Al foil to be heated by the protons. (b) Corresponding streak camera images showing space- and time-resolved thermal emission at $570\ \text{nm}$ from the rear side of the proton-heated foil. The streak camera images an $800\ \mu\text{m}$ spatial region with a 1 ns temporal window.

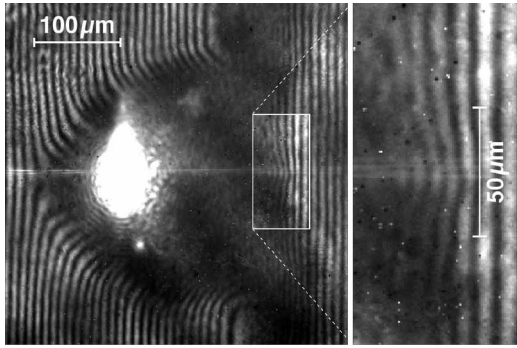


FIG. 2. Interferogram of focusing target shot taken 180 ps after incidence of the main pulse. The enlarged image on the right shows an approximately $50\ \mu\text{m}$ region of expanding plasma originating from the rear surface of the proton heated foil.

interferogram for the $320\ \mu\text{m}$ hemispherical shell target corresponding to the same shot shown in Fig. 1(b). The large fringe shifts on the left of the target arise from the blowoff plasma covering the outer surface of the hemispherical shell (the laser is incident from the left). The right side of the image corresponds to the rear surface of the secondary foil. A small region of expanding plasma is clearly visible. The plasma, originating from the rear surface, is centered along the central axis of the hemisphere, and extends laterally over approximately $50\ \mu\text{m}$, in good agreement with the $46\ \mu\text{m}$ heated region measured with the streak camera. Taken together these observations provide a strong indication of the ballistic

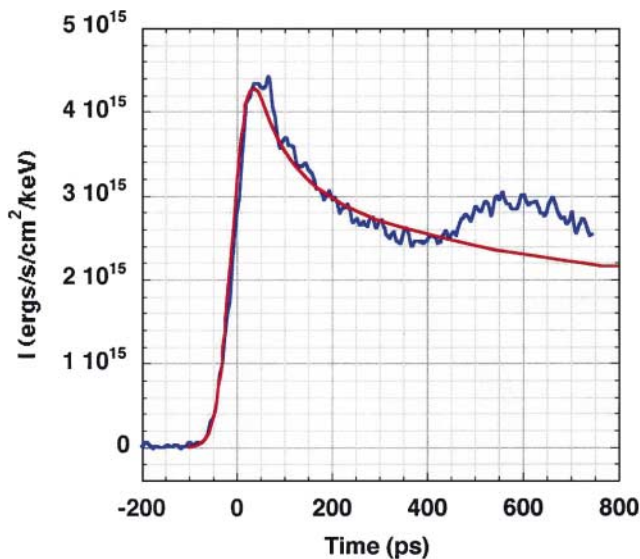


FIG. 3 (color). Comparison of time-dependent experimental (blue) and simulated (red) emission intensities for a hemispherical target shot. The experimental curve is a temporal line out spatially integrated over the $46\ \mu\text{m}$ FWHM of the signal. The simulated curve is a LASNEX calculation of the $570\ \text{nm}$ emission from a $23\ \text{eV}$ solid density Al plasma.

focusing of the proton beam, and of the corresponding enhancement in its flux density.

An absolute single wavelength intensity measurement of the rear surface emission enables us to estimate the rear side temperature of the proton heated foil. Absolute calibration of the streak camera and transmission optics in the beam path provided an overall accuracy of $\pm 25\%$. The radiation-hydrocode LASNEX [20] was used to model the hydrodynamic expansion and optical emission of the foil, assuming it to be instantaneously heated to some initial temperature. The simulated emission at $570\ \text{nm}$ from the rear surface was then compared with the absolute intensity measurements.

Taking line outs from the two images in Fig. 1(b) we obtain peak emission values of 5.7×10^{14} and $4.3 \times 10^{15}\ \text{ergs s}^{-1}\ \text{cm}^{-2}\ \text{keV}^{-1}$, respectively. Fitting to these peak values LASNEX modeling indicates for the planar heating case an initial temperature of the Al foil of $4 \pm 1\ \text{eV}$, and for the focused heating case a temperature of $23 \pm 6\ \text{eV}$. The comparison between experiment and simulation for this latter case is shown in Fig. 3. We note that the falloff in the emission intensity over the first 400 ps matches the data very closely. Since both the peak intensity and the falloff are strong functions of the plasma temperature, this good agreement gives us an added degree of confidence in the accuracy of the temperature measurement. The rise in signal at 400 ps may be due to gradient effects from the front of the foil such as a shock wave reaching the rear surface.

The proton beam flux required to heat the foils to the observed temperatures was estimated using a Monte Carlo simulation [21]. Protons with an exponential energy

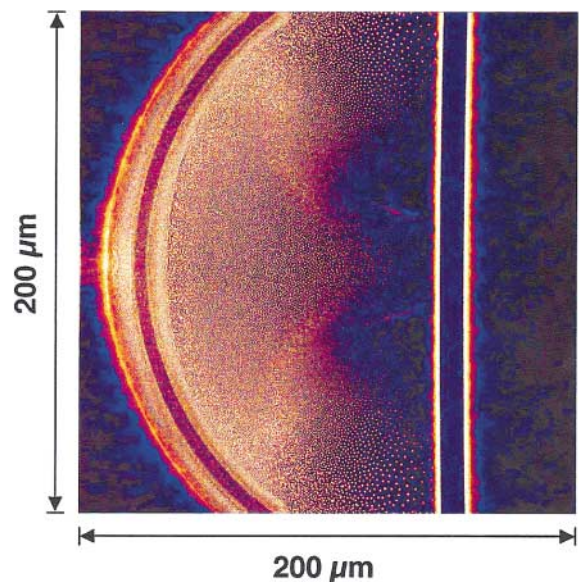


FIG. 4 (color). Particle-in-cell calculation of the electric field density at $3.4\ \text{ps}$ for a $5 \times 10^{18}\ \text{W cm}^{-2}$ intensity laser pulse incident on a $250\ \mu\text{m}$ diameter, $10\ \mu\text{m}$ thick hemispherical Al shell.

spectrum of 1.5 MeVKT were injected into a 10 μm thick Al foil. Energy loss and energy deposition as a function of distance were computed. The energy deposition at a depth of 10 μm was found to be 9.2×10^{-7} J/g per incident proton. Comparing to the evaluated energy density of 7.3×10^5 J/g at 23 eV [3] requires a total of 7.9×10^{11} protons focused to the observed 46 μm diameter spot. The total energy in such a distribution is 190 mJ, or 1.8% of the incident laser energy. Although approximate, this figure is entirely consistent with our previous estimates of a 1%–2% conversion efficiency to protons, showing that there is sufficient energy in the focused proton beam to induce isochoric heating to the level observed.

The focusing in a purely ballistic limit can be estimated by considering the flow angle deviation with source radius, as seen from a planar foil, and applying it to the hemispherical shell. The real behavior is expected to deviate from a pure ballistic case because of the spatiotemporal varying electron density and accelerating sheath field at the target rear surface. To gain insight into the complex focusing dynamics we carried out 2D particle-in-cell simulations which model the laser absorption, electron generation and propagation, and proton acceleration. A spatiotemporal Gaussian pulse with 50 μm and 100 fs FWHM, respectively, is incident at the left boundary of a $200 \times 200 \mu\text{m}^2$ simulation box. The resulting peak laser intensity is 5×10^{18} W cm^{-2} . The target consists of a 10 μm thick, 125 μm radius Al shell with a 10 μm thick flat Al foil positioned at the center of curvature of the shell. A 0.1 μm H layer is added to the inner surface of the hemisphere to simulate the proton-producing hydrocarbon layer. Figure 4 shows a result from the simulation, an electric field density map at a time 3.4 ps after the peak of the laser pulse. At this time the leading edge of the ion front has almost reached the rear foil. The accelerating sheath field can be seen to cover a large area of the inner surface of the hemisphere, producing a substantial degree of directed proton acceleration.

In conclusion, we have shown that an ultrashort-pulse beam of energetic protons, generated with a high-intensity laser pulse, is capable of isochorically heating a material to a warm dense plasma state at several eV. The protons volumetrically heat a 10 μm thick Al foil over an area of almost 200 μm in diameter. Using hemispherically shaped targets we have been able to generate a focused proton beam with a corresponding enhancement in flux of almost an order of magnitude. The focused

beam enabled heating of a localized 50 μm diameter area to 23 eV. We note that the 23 eV, 7.3×10^5 J/g solid density plasma reported herein was produced with a 10 J laser generating a 0.2 J proton beam; however, the world's largest subpicosecond lasers are capable of delivering laser energies of 500 J, and generating proton beams with up to 30 J, or 150 times the proton energy produced here [13,22]. Applying the techniques of proton heating and focusing at such facilities could enable isochoric heating of solid density plasmas to keV temperatures and gigabar pressures. This would open up new opportunities and directions in high energy-density physics and fusion energy research.

This work was funded under the auspices of the U.S. Department of Energy by LLNL under Contract No. W-7405-ENG-48.

-
- [1] B. A. Remington, D. Arnet, R. P. Drake, and H. Takabe, *Science* **284**, 1488–1493 (1999).
 - [2] J. Nuckolls, L. Wood, A. Thiessen, and G. Zimmerman, *Nature (London)* **239**, 139–142 (1972).
 - [3] R. M. More, K. H. Warren, D. A. Young, and G. B. Zimmerman, *Phys. Fluids* **31**, 3059–3078 (1988).
 - [4] K. S. Holian, LANL Report No. LA-10160-MS UC-34, 1984.
 - [5] G. W. Collins *et al.*, *Science* **281**, 1178 (1998).
 - [6] F. J. Rogers and C. A. Iglesias, *Science* **263**, 50–55 (1994).
 - [7] L. B. Da Silva *et al.*, *Phys. Rev. Lett.* **78**, 483 (1997).
 - [8] T. S. Perry *et al.*, *Phys. Rev. E* **54**, 5617–5631 (1996).
 - [9] J. J. MacFarlane *et al.*, *Phys. Rev. E* **66**, 046416 (2002).
 - [10] D. H. H. Hoffmann *et al.*, *Phys. Plasmas* **9**, 3651–3654 (2002).
 - [11] P. Audebert *et al.*, *Phys. Rev. Lett.* **89**, 265001 (2002).
 - [12] E. Clark *et al.*, *Phys. Rev. Lett.* **84**, 670–673 (2000).
 - [13] R. Snavely *et al.*, *Phys. Rev. Lett.* **85**, 2945–2948 (2000).
 - [14] M. Borghesi *et al.*, *Phys. Plasmas* **9**, 2214 (2002).
 - [15] A. J. Mackinnon *et al.*, *Phys. Rev. Lett.* **88**, 215006 (2002).
 - [16] S. P. Hatchett *et al.*, *Phys. Plasmas* **7**, 2076–2082 (2000).
 - [17] S. C. Wilks *et al.*, *Phys. Plasmas* **8**, 542–549 (2001).
 - [18] J. D. Bonlie, F. Patterson, D. F. Price, B. White, and P. T. Springer, *Appl. Phys. B* **70**, S155–S160 (2000).
 - [19] T. E. Cowan and H. Ruhl (to be published).
 - [20] G. B. Zimmerman and W. L. Kruer, *Comments Plasma Phys. Controlled Fusion* **2**, 51 (1975).
 - [21] J. F. Ziegler, J. P. Biersack, and U. Littmark, *The Stopping and Range of Ions in Solids* (Pergamon Press, New York, 1996).
 - [22] M. D. Perry *et al.*, *Opt. Lett.* **24**, 160–162 (1999).